CHARACTERISTICS AND THE STABLE NEBULIZATION OF A MOLECULE AGAINST SARS-CoV-2

Alice Lily Ma

A thesis submitted to the faculty at the University of North Carolina at Chapel Hill in partial fulfillment of the requirements for the degree of Master of Science in the Department of Biomedical Engineering.

Chapel Hill
2021

Approved by:

Samuel K. Lai

David A. Zaharoff

Raymond J. Pickles

ABSTRACT

Alice Lily Ma: Characteristics and the Stable Nebulization of a Molecule Against SARS-CoV-2
(Under the direction of Samuel K. Lai)

The SARS-CoV-2 virus, the causative agent of COVID-19, emerged at the end of 2019 and since then has created a massive global pandemic, with over 220 million cases and more than 4 million deaths worldwide. Though effective vaccines and treatments have been introduced, variants and mutations of the virus continue to emerge and evade current therapeutics, thus necessitating a need for an effective viral therapy that is able to neutralize SARS-CoV-2 and its variants. We developed an ACE2-linker-Fc molecule that is not only able to bind the wild type SARS-CoV-2 S protein with high, picomolar affinity, but is also able to bind to several variants of the virus, as well. This molecule is also able to be stably nebulized using a commercial vibrating mesh nebulizer, lending to its capability of being an effective inhaled immunotherapy for SARS-CoV-2, its current and future variants, as well as other similar respiratory viruses.

This work is dedicated to my parents, whose hard work and sacrifices led me here, and to Ricky, who supported me every step of the way.

ACKNOWLEDGMENTS

My graduate school journey has been one filled with ups and downs, happiness and hopelessness, successes and failures, yet the experience has inarguably changed me for the better, and I am grateful for it. I want to first and foremost thank my advisor, Dr. Sam Lai, for taking a chance on me, fresh out of my undergraduate studies and with not nearly enough of my abilities proven. Dr. Lai has funded me these past few years and given me the freedom to pursue the science that interests me. He has provided all the resources that have made me into the scientist I am today, and in times of need, he has shown incredible kindness and understanding. I am forever grateful and appreciative of his guidance, his mentorship, and his compassion. I also want to give thanks to my committee members, Dr. David Zaharoff and Dr. Ray Pickles, who did not hesitate to agree to be on my committee, and who have put in the time and effort to ensure I made it through to the end.

I want to acknowledge and give a special thanks to Dr. Ian Stewart from RTI International, whose nebulization work makes my entire second chapter possible. The experiments he carried out were not only of a high quality, but were done in such a timely manner, as well. He never hesitated to provide information or clarity, and I thank him for being such a foundation for a part of my work.

My time in the the Lai Lab and my achievements could not have been possible without the teamwork and assistance of my fellow colleagues: Dr. Karthik Tiruthani, Dr. Carlos Cruz-Teran, Dr. Limei Shen, Dr. Jasmine Edelstein, Dr. Justin Huckaby, Dr. Morgan McSweeney, Dr. Suruchi Shrestha, Dr. Anne Talkington, Dr. Jennifer Schiller, Zhongbo Li, Alison Schaefer,

Peter Voorhees, Marshall Fritz, Whitney Wolf, and Barbara Bell. Thank you to Dr. Limei Shen for being such a comforting, bright, and joyous figure to me and feeding me the best homemade food! And thank you to Barbara Bell who made sure I and other students were happy, taken care of, and on the right track for our own personal goals. I am grateful to Dr. Jasmine Edelstein, as well, for being one of the first people to take me under her wing when I first joined the lab and for teaching me all about grad school, lab, and life. Finally, a special thanks goes to Dr. Karthik Tiruthani and Dr. Carlos Cruz-Teran who fielded my never-ending questions and who so diligently and kindly trained me in most of the techniques that I utilized for this thesis. Without them and all the other wonderful people from the Lai Lab, I would not be where I am today.

Finally, I have to thank my family and friends for the support that led me to graduate school and all the way through graduate school. I am eternally grateful for the friendships and the relationships I made during my time here at UNC, and North Carolina will always hold a special place in my heart.

TABLE OF CONTENTS

LIST OF FIGURES

LIST OF ABBREVIATIONS

AAD	adaptive aerosol delivery
ACE2	angiotensin-converting enzyme 2
ALI	air-liquid interface
AM	airway mucus
C_{max}	maximum serum concentration of a drug (after administration)
CH	constant heavy chain (on an antibody)
COPD	chronic obstructive pulmonary disease
COVID-19	coronavirus disease 2019
DPI	dry powder inhaler
EC_{50}	half maximal effective concentration
ELISA	enzyme-linked immunoassay
EUA	Emergency Use Authorization (by the FDA)
Fab	antigen-binding fragment (on an antibody)
Fc	fragment crystallizable region (on an antibody)
FDA	United States Food and Drug Administration
G	glycine
IgG	immunoglobulin G
mAb	monoclonal antibody
MDI	metered dose inhaler
MW	molecular weight
Native-PAGE	native (non-denaturing) polyacrylamide gel electrophoresis
NGI	Next Generation Impactor

PsV	pseudovirus
RBD	receptor binding domain
S	serine
S protein	SARS-CoV-2 spike protein
SARS-CoV-1	severe acute respiratory syndrome coronavirus
SARS-CoV-2	severe acute respiratory syndrome coronavirus 2
USP	United States Pharmacopoeia
VH	variable heavy chain (on an antibody)
VLP	virus-like particle
VMN	vibrating mesh nebulizer
WT	wild type

CHAPTER 1: CHARACTERISTICS AND STABILITY OF ACE2-LINKER-FC

1.1 Introduction

Severe acute respiratory disease syndrome coronavirus 2 (SARS-CoV-2), the causative agent of coronavirus disease 2019 (COVID-19), has created a massive pandemic, with over 220 million confirmed cases and over 4 million deaths worldwide, with those numbers still growing despite the introduction of several promising and effective vaccines and treatments[1]. The scale of the ongoing COVID-19 pandemic is one that has not been observed in over a century, and with new variants and mutations arising that are able to evade current vaccines and treatments, there is an urgent and critical need for antiviral therapies that can be effective towards SARS-CoV-2, its current and future variants, as well as other coronaviruses and similar respiratory viruses[2,3].

SARS-CoV-2 is a membrane-enveloped virion that possesses an array of homotrimers of spike (S) glycoproteins on its surface[4]. It is the receptor binding domain (RBD) of these S proteins that mediate SARS-CoV-2 entry into human cells, when the RBD of the S protein binds to angiotensin-converting enzyme 2 (ACE2) on the target cell's surface[5]. With the S protein being the major antigenic target on the virus for neutralizing or protective antibodies, several research groups have aimed to utilize and take advantage of SARS-CoV-2's ACE2-tropism, by fabricating ACE2-Fc decoys that are able to neutralize the virus[6-8]. In general, this was carried out by either linking the entire ACE2 molecule to human IgG1-Fc[9-12] or linking just the extracellular section of ACE2 to human IgG1-Fc[6, 13-16]. However, S proteins unfortunately only bind with a moderate affinity to ACE2, so these ACE2-decoys also possessed only modest neutralizing capabilities[6,7]. Thus, we sought out to improve the binding capacity of wildtype

(WT) ACE2 to the virus. Through cryo-electron microscopy, it is known that for SARS-CoV-1, an earlier coronavirus similar in structure to SARS-CoV-2, that around 50-100 S proteins are present on the virion surface, with an average of ~15nm between proteins[17]. Even within individual homotrimer S proteins, there exists a considerable distance between any two of the three S proteins, which thus limits the ability of a singular antibody or ACE2-conjugate to bind to two different S proteins simultaneously. In order to increase the likelihood of bivalent binding of separate S proteins, we created what we termed an ACE2-linker-Fc (ACE2-$(G_4S)_6$-Fc) molecule. To create this molecule, we replaced the VH-CH1 domain of the standard IgG1 Fab with the extracellular segment of ACE2 and then also included a 30 amino acid flexible linker between the ACE2 portion and CH2[18]. This flexible linker was designed and intended to expand the reach and range of the molecule, thus increasing binding affinity.

In this chapter, the ACE2-linker-Fc molecule is analyzed and characterized and is shown to be able to bind to several different variants of SARS-CoV-2 S proteins, as well as whole, inactivated SARS-CoV-2 virus, virus-like particles (VLPs), and pseudoviruses representing variants of SARS-CoV-2 virions. In addition, the ACE2-linker-Fc molecule is shown to be structurally stable and able to retain binding affinity for over 35 days when stored at 4^{o}C. ACE2-linker-Fc, as well, does not significantly lose binding affinity when binding occurs at human body temperature (37^{o}C), lending to its ability to be a promising antiviral therapeutic candidate for treating SARS-CoV-2, its variants, and other emerging viruses that employ ACE2 as an entry receptor.

1.2 Materials and Methods

1.2.1 ELISAs

1.2.1.1 S protein ELISAs

S protein ELISA binding assays were performed using 96 well half-area plates (Fisher Scientific, Costar 3690) coated with 0.5ug/mL of S protein and incubated overnight at 4ºC. ELISA plates were blocked the following day with 5% (w/v) milk (LabScientific MSPP-M0841) with Tween 20 (Fisher Scientific BP337-100) at a 1:2000 dilution at room temperature for one hour. Samples were diluted in 1% (w/v) milk with Tween 20 at a 1:10,000 dilution and plated once the blocking had commenced and the 5% milk had been discarded. Samples were incubated at room temperature for 1hr, and the solution was discarded after the 1hr incubation. Plates were then washed with PBS containing Tween 20 at a 1:2000 dilution four times. A peroxidase-conjugated goat anti-human IgG Fc antibody (Rockland 709-1317) was diluted in 1% milk with Tween 20 at a 1:5000 dilution, plated, and incubated at room temperature for 1hr. The solution was then discarded and washed with PBS with Tween 20 two times, followed by washing with just PBS two more times. Plates were developed with TMB solution (ThermoFisher 34029), and development was stopped by adding 2N HCl (Sigma-Aldrich 320331). The absorbance at 450nm and 595nm was then measured with a microplate photodetector (Fisher Scientific, accuSkan FC).

1.2.1.2. Pseudovirus ELISAs

Pseudovirus ELISA binding assays were performed using 96 well half-area plates (Fisher Scientific, Costar 3690) coated with 0.05uL pseudovirus/well and incubated overnight at 4ºC. ELISA plates were blocked the following day with 5% (w/v) milk

(LabScientific MSPP-M0841) with Tween 20 (Fisher Scientific BP337-100) at a 1:2000 dilution at room temperature for one hour. Samples were diluted in 1% (w/v) milk with Tween 20 at a 1:10,000 dilution and plated once the blocking had commenced and the 5% milk had been discarded. Samples were incubated at room temperature for 1hr, and the solution was discarded after the 1hr incubation. Plates were then washed with PBS containing Tween 20 at a 1:2000 dilution four times. A peroxidase-conjugated goat anti-human IgG Fc antibody (Rockland 709-1317) was diluted in 1% milk with Tween 20 at a 1:5000 dilution, plated, and incubated at room temperature for 1hr. The solution was then discarded and washed with PBS with Tween 20 two times, followed by washing with just PBS two more times. Plates were developed with TMB solution (ThermoFisher 34029), and development was stopped by adding 2N HCl (Sigma-Aldrich 320331). The absorbance at 450nm and 595nm was then measured with a microplate photodetector (Fisher Scientific, accuSkan FC).

1.2.1.3 Inactivated whole virus ELISAs

The following reagent was deposited by the Centers for Disease Control and Prevention and obtained through BEI Resources, NIAID, NIH: SARS-Related Coronavirus 2, Isolate USA-WA1/2020, Heat Inactivated, NR-52296. Inactivated whole virus ELISA binding assays were performed using 96 well half-area plates (Fisher Scientific, Costar 3690) coated with 1uL inactivated whole virus/well and incubated overnight at 4^{o}C. ELISA plates were blocked the following day with 5% (w/v) milk (LabScientific MSPP-M0841) with Tween 20 (Fisher Scientific BP337-100) at a 1:2000 dilution at room temperature for one hour. Samples were diluted in 1% (w/v) milk with Tween 20 at a 1:10,000 dilution and plated once the blocking had commenced and the

5% milk had been discarded. Samples were incubated at room temperature for 1hr, and the solution was discarded after the 1hr incubation. Plates were then washed with PBS containing Tween 20 at a 1:2000 dilution four times. A peroxidase-conjugated goat anti-human IgG Fc antibody (Rockland 709-1317) was diluted in 1% milk with Tween 20 at a 1:5000 dilution, plated, and incubated at room temperature for 1hr. The solution was then discarded and washed with PBS with Tween 20 two times, followed by washing with just PBS two more times. Plates were developed with TMB solution (ThermoFisher 34029), and development was stopped by adding 2N HCl (Sigma-Aldrich 320331). The absorbance at 450nm and 595nm was then measured with a microplate photodetector (Fisher Scientific, accuSkan FC).

1.2.1.4 VLP ELISAs

VLP ELISA binding assays were performed using 96 well half-area plates (Fisher Scientific, Costar 3690) coated with 0.25uL Cov2 gag mCherry/well and incubated overnight at 4ºC. ELISA plates were blocked the following day with 5% (w/v) milk (LabScientific MSPP-M0841) with Tween 20 (Fisher Scientific BP337-100) at a 1:2000 dilution at room temperature for one hour. Samples were diluted in 1% (w/v) milk with Tween 20 at a 1:10,000 dilution and plated once the blocking had commenced and the 5% milk had been discarded. Samples were incubated at room temperature for 1hr, and the solution was discarded after the 1hr incubation. Plates were then washed with PBS containing Tween 20 at a 1:2000 dilution four times. A peroxidase-conjugated goat anti-human IgG Fc antibody (Rockland 709-1317) was diluted in 1% milk with Tween 20 at a 1:5000 dilution, plated, and incubated at room temperature for 1hr. The solution was then discarded and washed with PBS with Tween 20 two times, followed by washing with just

PBS two more times. Plates were developed with TMB solution (ThermoFisher 34029), and development was stopped by adding 2N HCl (Sigma-Aldrich 320331). The absorbance at 450nm and 595nm was then measured with a microplate photodetector (Fisher Scientific, accuSkan FC).

1.2.1.5 37°C ELISAs

Two ELISAs were carried out at the same time in order to analyze if there would be a difference between binding affinity at 25°C (RT) and 37°C. ELISA binding assays were performed using 96 well half-area plates (Fisher Scientific, Costar 3690) coated with 0.5ug/mL of S protein and incubated overnight at 4ºC. ELISA plates were blocked the following day with 5% (w/v) milk (LabScientific MSPP-M0841) with Tween 20 (Fisher Scientific BP337-100) at a 1:2000 dilution at room temperature for one hour. Samples were diluted in 1% (w/v) milk with Tween 20 at a 1:10,000 dilution and plated once the blocking had commenced and the 5% milk had been discarded. Samples were incubated at room temperature for 2hr or at 37°C for 2hr, and the solution was discarded after the 2hr incubation. Plates were then washed with PBS containing Tween 20 at a 1:2000 dilution four times. A peroxidase-conjugated goat anti-human IgG Fc antibody (Rockland 709-1317) was diluted in 1% milk with Tween 20 at a 1:5000 dilution, plated, and incubated at room temperature for 1hr. The solution was then discarded and washed with PBS with Tween 20 two times, followed by washing with just PBS two more times. Plates were developed with TMB solution (ThermoFisher 34029), and development was stopped by adding 2N HCl (Sigma-Aldrich 320331). The absorbance at 450nm and 595nm was then measured with a microplate photodetector (Fisher Scientific, accuSkan FC).

1.2.2 Native-PAGE gels

Samples were prepared using the NativePAGE Sample Prep Kit (ThermoFisher, Invitrogen BN2008). 5ug of sample was mixed with 2.5uL of 4X Sample Buffer, 0.5uL 5% G-250 Sample Additive, and water to fill up to 10uL. The 10uL per sample was loaded into the wells of a NativePAGE 3 to 12%, bis-tris, 1.0mm, mini protein gel (ThermoFisher, Invitrogen BN1001BOX) and this gel was then inserted into a protein gel box. 10uL of NativeMark Unstained Protein Standard (ThermoFisher, Invitrogen LC0725) is loaded as the ladder. 1X NativePAGE Dark Blue Cathode Buffer was added to the upper cathode buffer chamber, and 1X NativePAGE Anode Buffer was added to the lower anode buffer chamber. 1X NativePAGE Dark Blue Cathode Buffer was made by adding 50mL of 20X NativePAGE Running Buffer (ThermoFisher, Invitrogen BN2001) and 50mL 20X NativePAGE Cathode Additive (ThermoFisher, Invitrogen BN2002) to 900mL DI water. 1X NativePAGE Anode Buffer was made by adding 50mL of 20X NativePAGE Running Buffer to 950mL DI water.

The gel is then run at 150V for 1h30m. After run time is completed, the gel is extracted and is placed in 100mL Fix solution (40% methanol (Fisher, 412-4), 10% acetic acid (Fisher, A38-212)) and microwaved for 45s. The gel is placed on a shaker and shaken for 15m at RT, after which the Fix solution is discarded. 100mL of Destain Solution (8% acetic acid) is added and microwaved for 45s. The gel is then shaken at room temperature for 1h and then imaged on a white screen.

1.3 Results

1.3.1 Binding of ACE2-linker-Fc to S protein

The ACE2-$(G_4S)_6$-Fc, or ACE2-linker-Fc, molecule was one that had previously been designed and produced in-house. The estimated distance between RBDs on the same SARS-CoV-2 spike (S) protein range from 60 to 100 Å when all three RBDS are in the "up" conformation[18]. Thus, in order to span that distance, as well as to add flexibility to the molecule, a $(GGGGS)_6$ flexible linker with a length of ~10nm was added in between the extracellular ACE2 fragment and the IgG1-Fc of ACE2-Fc decoys that several other groups had previously fabricated[18] (Figure 1.1A). This flexible linker thus allows for bivalent binding of the S protein to occur, and since the linker resides on each of the two heavy chains, the two ACE2 fragments of ACE2-linker-Fc can theoretically extend distances nearly twice the linker length (Figure 1.1B)[18]. Through size exclusion chromatography/multi-angle light scattering (SEC/MALS), the molecular weight (MW) of ACE2-linker-Fc is ~212 kDa[18]. The molecule is largely found in its monomeric form (~91%) after protein A purification, with aggregates and oligomers of the protein making up the remainder[18].

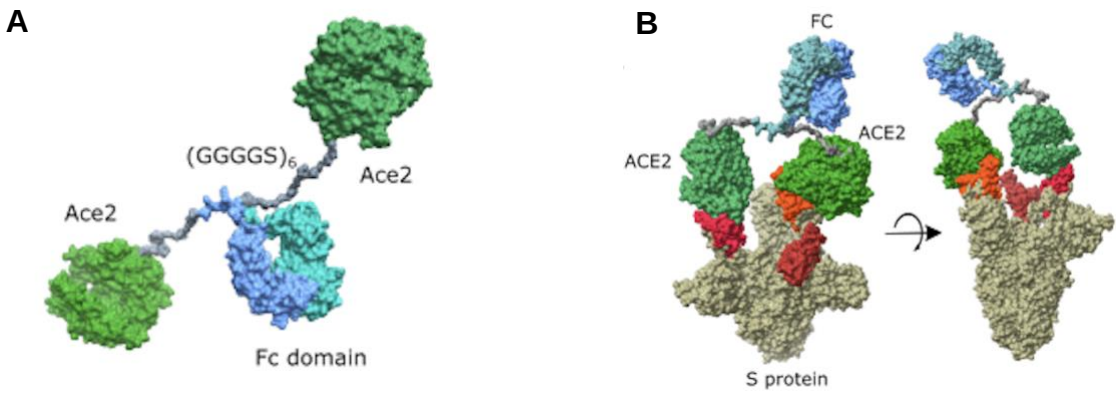

Figure 1.1 Computational models of ACE2-linker-Fc and its binding to S protein
A) ACE2 extracellular fragment linked to human IgG1-Fc with a 30 amino acid glycine-serine flexible linker (ACE2-$(G_4S)_6$-Fc). The flexible linker is shown in gray and allows for an extended reach of the ACE2 domains on the S protein.
B) ACE2-linker-Fc bivalently binding to two ACE2 domains on the SARS-CoV-2 S protein, which would not be possible without the flexible linker. The three RBDs per S protein are shown in shades of red.

Reprinted from Tiruthani, K. *et al.* Engineering a "muco-trapping" ACE2-immunoglobulin hybrid with picomolar affinity for topical immunotherapy against SARS-CoV-2. To be submitted; used with permission

To assess the ability of ACE2-linker-Fc to bind to the SARS-CoV-2 S protein, we first carried out an ELISA to measure the binding affinity of the molecule to the S protein of WT strain USA-WA1/2020. We also included ACE2-Fc as well as full length ACE2-decoy (ACE2(740)-Fc, abbreviated as 208[9]). It was consistenly shown that among the three ACE2-decoys that were tested, ACE2-linker-Fc showed the highest binding affinity (Figure 1.2A). ACE2-linker-Fc exhibited picomolar EC_{50}, with a mean of 246 pM, while in contrast, ACE2-Fc and 208 possessed a mean EC_{50} of 10.49 nM and 15.12 nM, respectively (Figure 1.2B). These results show that ACE2-linker-Fc binds to the WT SARS-CoV-2 S protein with a significantly higher binding affinity than other ACE2-decoys and underlines the ability of the molecule to be an effective protein therapeutic.

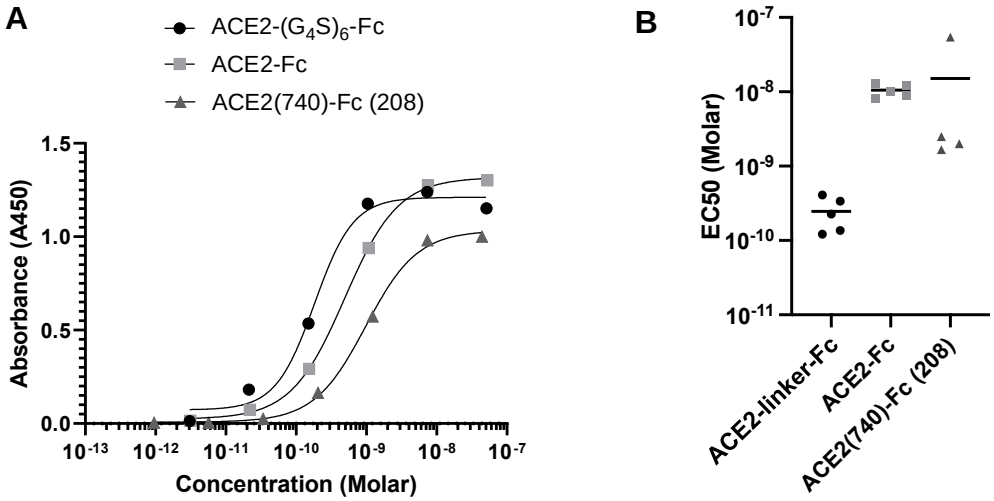

Figure 1.2 ELISAs of ACE2-decoys binding to WT SARS-CoV-2 S protein
A) ELISA binding curves comparing ACE2-linker-Fc to ACE2-Fc and ACE2(740)-Fc (208). B) Molar EC_{50}s of ELISA curves are plotted, and the mean is designated with a line. ACE2-linker-Fc, ACE2-Fc, and 208 are shown to possess mean EC_{50}s of 246 pM, 10.49 nM, and 15.12 nM, respectively.

1.3.2 Structural and molecular stability of ACE2-linker-Fc

Now that it had been shown that ACE2-linker-Fc bound to WT SARS-CoV-2 S protein with high, picomolar affinity, we wanted to determine the stability of the molecule at 4^{o}C over time. We carried out a stability study, which involved performing Native-PAGE and ELISA every 7 days for 35 days, in order to assess potential changes or losses in protein structure, conformation, and binding affinity. The ACE2-linker-Fc molecule resides in buffer that is comprised of 20 mM His, 20 mg/mL sucrose, 0.2% polysorbate 80, 130 mM NaCl, and is pH-adjusted to 6.2.

Across the 35 days, it was shown that the ACE2-linker-Fc protein retained its structure and conformation and also did not present significant changes in its binding affinity (Figure 1.3). The ACE2-linker-Fc molecule presents as a single band on Native-PAGE, displaying that there

are no aggregates, and confirming its monomeric form. The protein runs at a MW of ~350 kDa, and throughout the 35 days, the ACE2-linker-Fc molecule ran as a single band at ~350 kDa, suggesting that the molecule has not sustained any substantial molecular or structural changes, and also has not significantly aggregated in solution (Figure 1.3A). The ELISAs performed throughout the 35-day stability study show that binding affinity is not significantly altered or decreased throughout the 5-week study, with the EC_{50} beginning at 0.97 nM and ending at 1.24 nM, indicating only a very slight decrease in binding affinity that is not statistically significant (Figure 1.3B-C). These results are promising, in that they show that the ACE2-linker-Fc molecule is stable at 4^{o}C for over one month, lending to the practicality and ease of storage and usage of the protein.

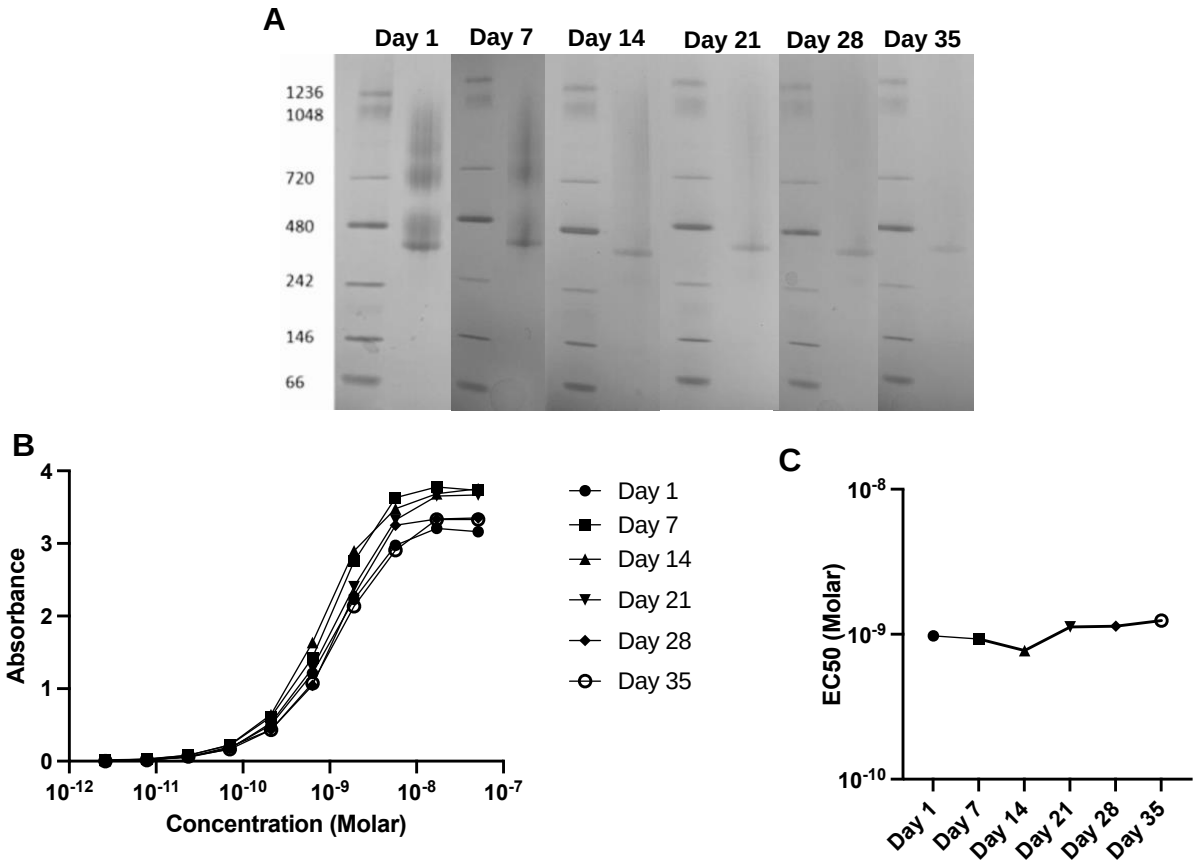

Figure 1.3 Stability assays of ACE2-linker-Fc at 4ºC
A) Native-PAGE of ACE2-linker-Fc in buffer at 4ºC, performed every week for 5 weeks. The values on the leftmost side displays the MW in kDa. The protein ran as a single band at the same MW (~350kDa) for all 5 weeks and also did not show signs of aggregation or structural changes. B) ELISA binding curves of ACE2-linker-Fc. ELISAs were performed every week for 5 weeks. C) EC_{50}s of the curves shown in (B) are plotted. The beginning EC_{50} on Day 1 is 0.97 nM, while the ending EC_{50} on Day 35 is 1.24 nM, displaying a very slight decrease in binding affinity that is not statistically significant.

1 3.3 Binding of ACE2-linker-Fc to mutant S proteins

Next, we aimed to see if our ACE2-linker-Fc molecule was capable of binding different SARS-CoV-2 variants, since this is the major advantage of ACE2 decoys over conventional monoclonal antibodies (mAbs). Thus, we measured the molecule's binding affinity to B.1.1.7 (UK) and B.1.351 (SA) S proteins using ELISA. These two variants were some of the first to be identified and possess known escape mutations that may make these variants exempt from

vaccines and current therapeutics[19]. Both variants have ~50% increased transmission, and this is likely due to the mutations present in the S protein of the variants[20]. The N501Y mutation within the RBD that is seen in both the UK and SA variants may influence viral binding and aid the virus in infecting cells more efficiently and thus spreading more rapidly[21]. ACE2-linker-Fc was indeed able to bind these two variants with strong binding affinity, and the binding affinities were highly comparable, as well, with median EC_{50}s for WT, UK, and SA all falling between 310 and 550 pM (Figure 1.4A-B).

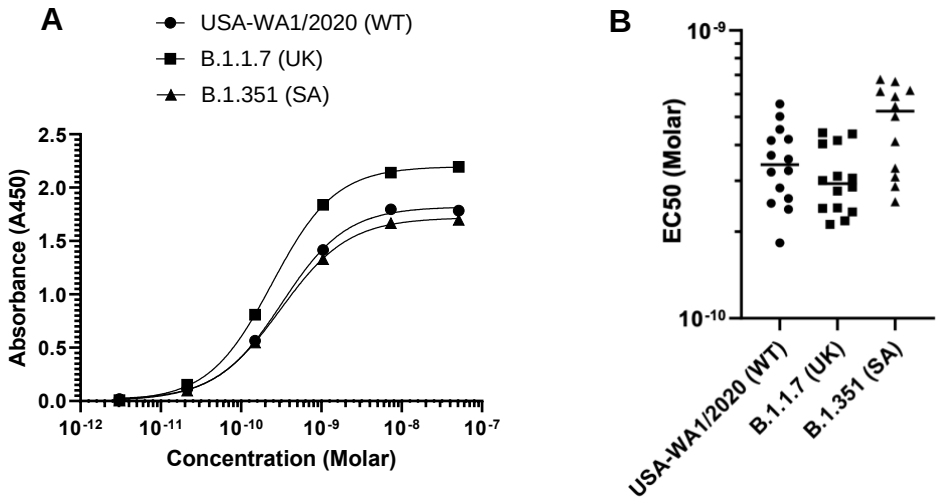

Figure 1.4 ACE2-linker-Fc binding to S protein variants
A) ELISA binding curves of ACE2-linker-Fc to USA-WA1/2020 (WT), B.1.1.7 (UK), and B.1.351 (SA) S proteins. ACE2-linker-Fc successfully binds WT and two variants with competent and comparable binding affinity.
B) EC_{50}s of ELISA results are plotted, with the median designated with a line. The median EC50s for WT, UK, and SA S proteins are highly comparable, with EC_{50}s for all falling between 310 and 550 pM.

For comparison, we also measured the binding ability of RGN10989, a mAb created by Regeneron that is included in its cocktail that received Emergency Use Authorization (EUA) by the FDA and that has recently been approved by Japan as the first country to allow the use of the cocktail for treatment of mild to moderate SARS-CoV-2 infection[22,23]. RGN10989 was able to

bind WT and UK S proteins with satisfactory and comparable binding affinity to ACE2-linker-Fc, however, it failed to bind to the SA S protein (Figure 1.5). These results underline the effectiveness and utility of ACE2-linker-Fc to bind and neutralize current and inevitable future SARS-CoV-2 variants.

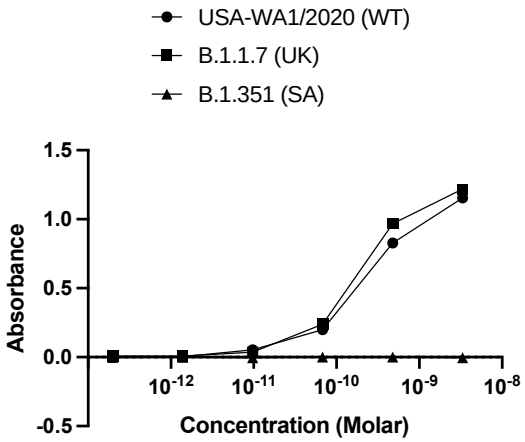

Figure 1.5 RGN10989 binding to S protein variants
RGN10989 mAb binds to USA-WA1/2020 (WT) and B.1.1.7 (UK) S proteins but fails to bind to B.1.351 (SA) variant S protein. The EC50s for the WT and UK binding curves are 255 pM and 195 pM, respectively.

1.3.4 Binding of ACE2-linker-Fc to inactivated whole virus, virus-like particle, and pseudoviruses

We next sought to evaluate whether ACE2-linker-Fc was able to bind to whole virus and other virus substitutes, as up to this point, we had only measured the ability of the molecule to bind to S protein. By altering a previously utilized virus-like particle (VLP) that had been designed to mimic HIV, we created a SARS-CoV-2-based lentivirus we termed Cov2 GAG mCherry (cotransfection of pGAG-mCherry plasmid and Cov2 S protein plasmid in 1:1 ratio) that had WT S protein present on the surface[24]. Using ELISA, we measured the binding affinity of ACE2-linker-Fc to the Cov2 gag mCherry VLP. ACE2-linker-Fc was able to bind the VLP with a high binding affinity (EC_{50}=728.7 pM) that was comparable to the binding affinities

obtained when binding occurred on just S proteins (Figure 1.6A). Next, we measured the binding affinity of ACE2-linker-Fc to pseudoviruses (PsVs) that had previously been shown to efficiently infect cells that expressed ACE2[20]. PsVs possessing WT, UK, and SA S proteins were created, and ELISAs were performed to assess binding affinity. ACE2-linker-Fc bound to all three PsVs with EC_{50}s of 150.1 nM, 32.83 nM, and 19.11 nM for WT, UK, and SA PsVs, respectively (Figure 1.6B). Finally, we obtained heat inactivated USA-WA1/2020 (WT) whole SARS-CoV-2 virus and performed an ELISA with ACE2-linker-Fc to once again assess binding affinity. The molecule was able to successfully bind to the inactivated whole SARS-CoV-2 virus with an adequate binding affinity, possessing an EC_{50} of 54.4 nM (Figure 1.6C).

These results show the promise and potential of ACE2-linker-Fc being a functional and practical protein therapeutic, as it is not only able to bind just S protein with high binding affinity, but also virus substitues and even inactivated whole SARS-CoV-2 virus with high, pico- and nanomolar affinity.

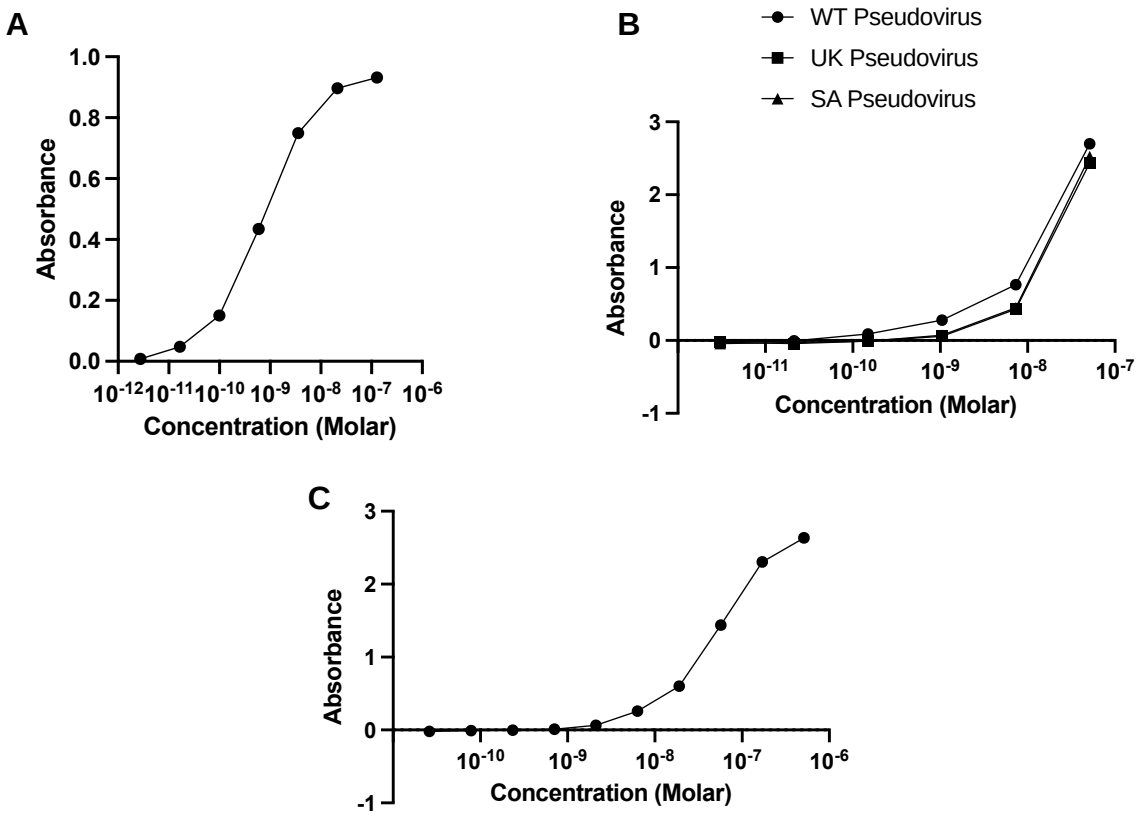

Figure 1.6 ACE2-linker-Fc binding to VLP, PsVs, and whole inactivated SARS-CoV-2 virus
A) ELISA binding curve of ACE2-linker-Fc to Cov2 GAG mCherry VLP. The EC_{50} of the curve is 728.7 pM.
B) ELISA binding curve of ACE2-linker-Fc to WT, UK, and SA PsVs. The EC_{50}s of the WT, UK, and SA curves are 150.1 nM, 842.8 nM, and 19.11 nM, respectively.
C) ELISA binding curve of ACE2-linker-Fc to inactivated whole WT SARS-CoV-2 virus. The EC_{50} of the curve is 54.4 nM.

1.3.5 Binding affinity of ACE2-linker-Fc at 37°C

Finally, as an additional measure of practicality, we conducted an ELISA at body temperature, 37°C, to assess whether binding affinity is altered or decreased at an appropriate physiological temperature. ACE2-linker-Fc binding affinity to WT S protein was evaluated in parallel at room temperature, 25°C, and at body temperature, 37°C, and it was found that the EC_{50}s for both were highly comparable (EC_{50} at 25°C=357.3 pM and at 37°C=951.3 pM) (Figure

1.7A-B). Though the binding affinity at 37°C was lower than at 25°C, the decrease was slight and not statistically significant, and still presented a very adequate binding affinity.

Thus, if ACE2-linker-Fc were present in the human body, its binding affinity would not be impeded by the higher temperatures present in the body. These results lend more precedence to the suggestion that ACE2-linker-Fc may be an effective, practical, and realistic therapeutic for treating SARS-CoV-2.

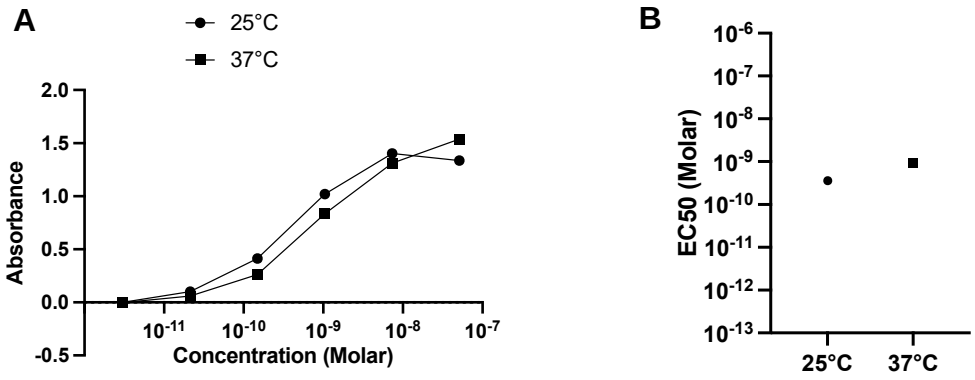

Figure 1.7 ACE2-linker-Fc binding to WT S protein at 25°C versus 37°C
A) ELISA binding curves of ACE2-linker-Fc binding to WT S protein at 25°C and 37°C.
B) The EC_{50}s of the binding curves in (A) are plotted. The EC_{50}s of binding occurring at 25°C and 37°C are 357.3 pM and 951.3 pM, respectively (SD=0.30 nM).

1.4 Discussion

Here we have analyzed and characterized the ACE2-linker-Fc (ACE2-$(G_4S)_6$-Fc) molecule that may serve to be an effective, efficient, and practicle protein therapeutic against SARS-CoV-2. Though there have been many neutralizing mAbs that have been identified and even several that have received Emergency Use Authorization (EUA) by the FDA, these mAbs are proven to be ineffective against viral escape mutants. Though these neutralizing mAbs also possess high, picomolar binding affinities to S protein and have been shown to be effective at preventing serious SARS-CoV-2 infection, their neutralizing abilities are entirely lost when

presented with a mutated virus variant. These mutated variants, however, still retain ACE2 binding ability.

In an effort to avoid escape mutants, some groups have chosen to focus on cocktails of neutralizing mAbs that target distinct structural epitopes of the SARS-CoV-2 virus. Though the possibility of viral escape is indeed reduced through utilizing this combination approach, the opportunity of viral mutants to escape both or all mAbs comprising the cocktail still exists. For instance, a single amino acid mutation (E406W) rendered the Regeneron REGN-COV2 cocktail that received EUA by the FDA ineffective, even though both mAbs in the cocktail targeted different, distinct structural epitopes[25]. In another occurrence, Eli Lilly's mAb cocktail, currently in phase III clinical trials, displayed a >45-fold and >511-fold decline in pseudovirus neutralization potency against the South African (B.1.351) and Brazil (P.1) variants, respectively[18].

Considering the highly prevalent issue of escape mutants, as well as the difficulties and tremendous efforts required to push a molecule through clinical trials, it became paramount to create one single mAb that could prevent viral escape. Molecules that target ACE2, or ACE2-decoys, are able to bind to, and thus neutralize, all viruses that utilize ACE2 as its entry receptor, which includes SARS-CoV-2 along with its similarly highly contagious and pandemic-potential sister, SARS-CoV-1. Many groups have designed and produced their interpretations of ACE2-decoys, including engineering variants of ACE2 via mutant library screening[6,7,9], as well as creating dimeric, trimeric[16,26], and even tetrameric[13] ACE2-Fc molecules. Instead of focusing on joining multiple ACE2 fragments together, however, we shifted our attention to perfecting a length of linker between extracellular ACE2 and Fc, thus originating the 30 amino acid glycine-serine linker ($(G_4S)_6$).

The Fc portion of the ACE2-linker-Fc molecule design is purposeful, as well. The SARS-CoV-2 virus infects the apical side of airway epithelium (the airway lumen) and mainly sheds progeny viruses back into the airway mucus (AM) that coats the epithelium[27]. Due to this mechanism, crosslinking shed viruses to the mucins that make up AM may trap the virus in the mucin matrix until the mucus, along with the virus, is expelled either via natural mucociliary actions or via coughing[28]. Previous work from our group shows that the Fc domain of IgG1 possesses a weak affinity to mucins that, when enabled in large quantities, facilitates potent "muco-trapping" of viruses in mucus[28-30]. The ACE2-linker-Fc molecule can thus aid in the treatment of SARS-CoV-2 via binding and neutralization, as well as via muco-trapping mechanisms.

ACE2-linker-Fc has been shown to bind to WT SARS-CoV-2 S protein with a high 246 pM affinity, as well as being able to bind to the UK (B.1.1.7) and SA (B.1.351) variants with similar, high picomolar affinity. Not only does ACE2-linker-Fc bind to S protein with a strong affinity, but it is also able to bind to SARS-CoV-2 virus substitutes (VLP and variant PsVs), as well as inactivated whole SARS-CoV-2 virus (EC_{50}=54.4 nM) with nanomolar affinity. The molecule is stable in solution at 4^{o}C and retains its structural and molecular composition after 35 days, and binding affinity is also not significantly reduced within those 5 weeks. In addition, binding affinity of ACE2-linker-Fc to WT S protein is not significantly decreased when binding occurs at body temperature, 37^{o}C, lending to the potential of the molecule to retain effective binding and neutralization capacity when administered in the body. Further data on neutralization and *in vivo* work that has been collected by our group that will be submitted for publication soon shows more promise for the realistic efficacy of ACE2-linker-Fc: ACE2-linker-Fc neutralizes SARS-CoV-2 pseudovirus with an average IC_{50} of 52 ng/mL, which is a nearly 5-

fold and 6-fold greater potency than ACE2-Fc and ACE2(740)-Fc (208), respectively[18]. Neutralization potency of ACE2-linker-Fc has also shown to be very promising when evaluated with live SARS-CoV-2 WT and variants, as well[18]. ACE2-linker-Fc has also shown to have *in vivo* success, with treatment of the molecule resulting in a ~10-fold reduction in viral load in the nasal turbinate tissues of hamsters[18].

These results emphasize the advantages, high effectiveness, and practicality of the ACE2-linker-Fc molecule in treating SARS-CoV-2 infections. Not only is this molecule a compelling candidate for treating SARS-CoV-2, however, the molecule is capable of almost universal ACE2 target treatment, due to its deliberate and intentional design. This molecule can benefit from more testing with additional variants, especially the Delta variant (B.1.617.2) that has recently become of high interest due to its ability to evade current authorized vaccines and treatments. In addition, more *in vivo* work is ongoing, as well. The matter of how best to administer the ACE2-linker-Fc molecule is also a crucial topic to examine, one which will be discussed further in the following chapter.

CHAPTER 2: STABLE NEBULIZATION OF ACE2-LINKER-FC

2.1 Introduction

The delivery of proteins to the lung via nebulization has increasingly become of interest in the last two decades and has begun to be explored as an effective and advantageous method of administering therapeutics[31]. Protein therapeutics have historically been administered parenterally, though this systemic route approach has proven to be inefficient at delivering drugs to the lungs[32]. Protein therapeutics also cannot withstand oral ingestion, as the harsh pH environment of the gastrointestinal tract degrades the protein[33]. Injectable formulations avoid the degradation and instability issues that are caused via the oral route, however, a high systemic concentration of the protein or antibody is required to achieve the desired therapeutic effects at the target location[34]. Thus, there remains an urgent need for therapeutics that deliver directly and locally to the lungs for increased efficacy in treating respiratory diseases.

Direct delivery of antibodies to the lungs allows for lower doses of inhaled protein to possess therapeutic results that are equivalent or even superior to the high doses that are required for systemic administration[35]. Though higher pulmonary levels of protein therapeutics can be accomplished through nebulization, there are some disadvantages that arise from drug administration via inhalation, one being that antibodies and other proteins are cleared from the lungs within 24 hours, whereas antibodies in the plasma can circulate for 3 weeks or more[36]. Nevertheless, nebulization is non-invasive, able to be self-administered, and has proven to be exceptionally safe, and as such, remains a viable and promising method of protein therapeutic administration[32,37].

Nebulizers are one of three primary categories of aerosol delivery systems – the other two being metered dose inhalers (MDIs) and dry powder inhalers (DPIs) – and have been preferred over other techniques due to the solubility of the protein and relatively straightforward and uncomplicated formulation[38,39]. Nebulizers create aerosol droplets from a liquid solution of the specific drug, and these nebulized formulations are also less expensive to manufacture and test, since the production process for these formulations does not include extra drying steps that formulations for other devices require[32,40]. However, prolonged storage of proteins in a liquid formulation can lead to instability issues, such as degradation and aggregation of the therapeutic protein[40]. Additionally, the process of nebulization requires the protein to be put under physical stresses, such as shearing forces and heat, as well as the air-liquid interface (ALI), which could also alter the conformation and structure of the protein through denaturation, chemical modification, and aggregation[31,32]. However, there are common and simple strategies for stabilizing liquid protein formulations (such as utilizing surfactants, sugars, and salts) to avoid aggregation and prolong protein stability in solution[41]. In addition, there exists nebulizer devices, such as vibrating mesh nebulizers (VMNs), that employ processes that do not change the solution temperature and also significantly reduce the amount of shear force and other physical stresses exerted on the protein, thus overcoming most of the shortcomings that are linked to nebulization[42].

Presently, over ten inhaled protein therapeutics are being evaluated in clinical trials (with one, Pulmozyme, on the market for treatment of cystic fibrosis) for an array of respiratory diseases, including asthma, cystic fibrosis, COPD, lung cancer, and COVID-19[31]. Certainly, since the rise of COVID-19, there has been an increased interest in the use of inhaled protein therapeutics for the treatment of viral respiratory diseases, and has raised the possibility of

treating COVID-19 with aerosol therapy[37]. In this chapter, we assess the ability of ACE2-linker-Fc to be stably nebulized with a vibrating mesh nebulizer, and its potential to be an effective therapeutic against SARS-CoV-2.

2.2 Materials and Methods

2.2.1 Glass impinger nebulization

Nebulization was carried out by Dr. Ian Stewart of RTI International. An Innospire Go (Philips, USA) vibrating mesh nebulizer was utilized. The glass twin impinger experiments were performed generally according to US Pharmacopeia (USP) methods[43]. The nebulizer was actuated and vacuum was pulled at 60 L/min for 1 min. In order to collect sufficient drug, the glass impinger was run dry without any collection liquid. After the 1 min experiment, the upper chamber and lower chamber were washed with 2 and 5 mL buffer respectively. Samples were stored at 4 °C until ready for analysis.

2.2.2 NGI nebulization

Nebulization was carried out by Dr. Ian Stewart of RTI International. An Innospire Go (Philips, USA) vibrating mesh nebulizer was utilized. Inertial Impaction was performed using a Next Generation Impactor (NGI; Copley, USA) generally following the procedure in USP <1601>[43]. Briefly, the nebulizer was loaded with the mAb solutions and attached to the inlet of the NGI via custom mouthpiece adaptor (made from silicone). A solenoid valve was connected in line between the NGI and vacuum pump and set for 60 seconds. Vacuum was pulled at 15 L/min. The nebulizer was actuated and the vacuum/solenoid was engaged. The aerosol from the nebulizer was deposited on the stages of the impactor and washed via appropriate buffer for 5 minutes. Samples were stored at 4 °C until assayed.

2.2.3 Native-PAGE gels with silver staining

Samples were prepared using the NativePAGE Sample Prep Kit (ThermoFisher, Invitrogen BN2008). 400ng of sample was mixed with 2.5uL of 4X Sample Buffer, 0.5uL 5% G-250 Sample Additive, and water to fill up to 10uL. The 10uL per sample was loaded into the wells of a NativePAGE 3 to 12%, bis-tris, 1.0mm, mini protein gel (ThermoFisher, Invitrogen BN1001BOX) and this gel was then inserted into a protein gel box. 10uL of NativeMark Unstained Protein Standard (ThermoFisher, Invitrogen LC0725) is loaded as the ladder. 1X NativePAGE Dark Blue Cathode Buffer was added to the upper cathode buffer chamber, and 1X NativePAGE Anode Buffer was added to the lower anode buffer chamber. 1X NativePAGE Dark Blue Cathode Buffer was made by adding 50mL of 20X NativePAGE Running Buffer (ThermoFisher, Invitrogen BN2001) and 50mL 20X NativePAGE Cathode Additive (ThermoFisher, Invitrogen BN2002) to 900mL DI water. 1X NativePAGE Anode Buffer was made by adding 50mL of 20X NativePAGE Running Buffer to 950mL DI water.

The gel is then run at 150V for 1h30m. After run time is completed, the gel is extracted. To carry out the silver staining, we utilized the Pierce Silver Stain Kit (ThermoFisher, 24612), where the manufacturer protocol is followed. The gel is then imaged on a white screen.

2.2.4 S protein ELISAs

S protein ELISA binding assays were performed using 96 well half-area plates (Fisher Scientific, Costar 3690) coated with 0.5ug/mL of S protein and incubated overnight at 4^{o}C. ELISA plates were blocked the following day with 5% (w/v) milk (LabScientific MSPP-M0841) with Tween 20 (Fisher Scientific BP337-100) at a 1:2000 dilution at room temperature for one hour. Samples were diluted in 1% (w/v) milk with Tween 20 at a 1:10,000 dilution and plated once the blocking had commenced and the 5% milk had been discarded. Samples were incubated

at room temperature for 1hr, and the solution was discarded after the 1hr incubation. Plates were then washed with PBS containing Tween 20 at a 1:2000 dilution four times. A peroxidase-conjugated goat anti-human IgG Fc antibody (Rockland 709-1317) was diluted in 1% milk with Tween 20 at a 1:5000 dilution, plated, and incubated at room temperature for 1hr. The solution was then discarded and washed with PBS with Tween 20 two times, followed by washing with just PBS two more times. Plates were developed with TMB solution (ThermoFisher 34029), and development was stopped by adding 2N HCl (Sigma-Aldrich 320331). The absorbance at 450nm and 595nm was then measured with a microplate photodetector (Fisher Scientific, accuSkan FC).

2.3 Results

2.3.1 Nebulization of ACE2-linker-Fc

There are three main classes of nebulizers: jet, ultrasonic, and mesh nebulizers, which produce aerosols via different physical processes, but all typically create droplets between 2 and 5 μm[44]. It has been shown that droplets possessing median mass aerodynamic diameters that fall between 4 and 5 μm provide the most effective deposition into the lung airways[45,46]. Jet and ultrasonic nebulizers, however, run into two considerable concerns. Both nebulizers employ several rounds of droplet recirculation in their nebulization process, which promotes protein aggregation and denaturation[47,48]. Aggregated proteins are a common concern with inhaled delivery, as they could potentially induce anti-drug antibodies, thus causing unwanted immunogenicity[49]. Both jet and ultrasonic nebulizers also possess a considerable amount of "dead volume," as well. Residual mass is around 30% of the actual loaded drug mass in ultrasonic nebulizers, and residual mass in jet nebulizers can reach 50%[50,51]. This substantial

amount of wasted volume and wasted drug product is extremely undesirable for efficacious drug delivery as well as the inevitable expensive cost of a protein therapeutic.

Vibrating mesh nebulizers (VMNs), in contrast, bypass these concerns. VMNs possess a vibrating mesh that is made up of conical holes, with the wider end on the liquid interface side. Aerosols are formed by pushing the liquid solution that contains the protein therapeutic through this vibrating mesh, with the resulting droplets being of a predictable size, since the diameter of droplets can be chosen and adjusted simply by changing the pore size of the vibrating mesh[52]. Unlike with jet and ultrasonic nebulizers, with VMNs, there is no need to recirculate the solution within the nebulizer, which greatly reduces the concerns of protein aggregation and denaturation[53]. VMNs have shown to facilitate excellent protein deposition in the lungs and also possess residual volumes of less than 10%[54]. As additional advantages, VMNs are small, portable, battery-powered, and easy-to-use.

For our purposes, we employed a Philips InnoSpire Go portable VMN to nebulize our ACE2-linker-Fc molecule. We nebulized the ACE2-linker-Fc molecule at two different concentrations, 10 mg/mL and 20 mg/mL. At 10 mg/mL, we collected the resulting aerosol droplets in a two-chamber (upper and lower) glass impinger setup, with the upper chamber capturing droplets > 6.4 μm and the lower chamber capturing droplets < 6.4 μm[55] (Figure 2.1A). At the 20 mg/mL concentration, we once again collected the resulting aerosols in the glass impinger, but this time, also collected in a different particle sizing instrument called a Next Generation Impactor (NGI). This stainless steel instrument possess 8 trays, or chambers, that capture droplets of a wider and more discrete range of particle sizes (from 0.24 μm to 14.10 μm)[56] (Figure 2.1B). These instruments are mainly utilized to determine aerosol particle sizes. However, for our purposes, we focused less on the sizing features of the instruments and more on

their utility as collection vessels, to ensure we were able to collect and analyze protein that had undergone nebulization. Thus, we proceeded to characterize the post-nebulized ACE2-linker-Fc that we recovered from the chambers of both instruments.

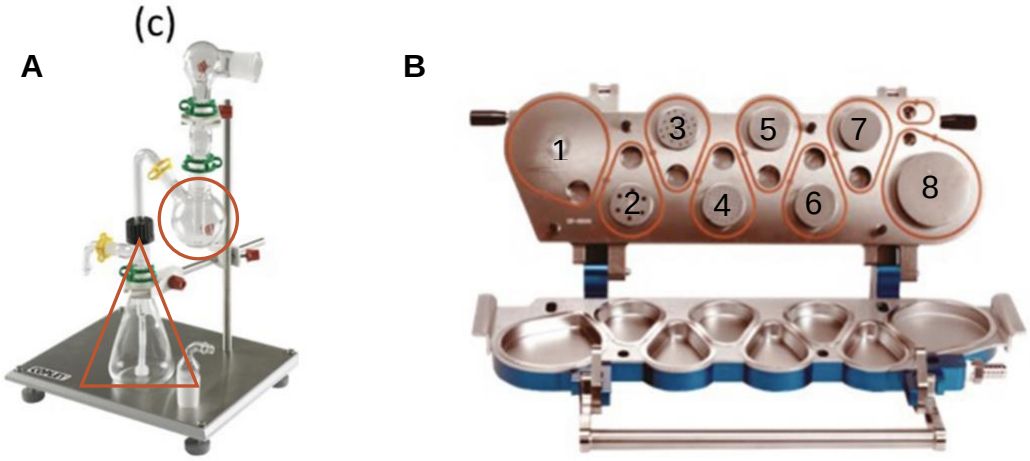

Figure 2.1 Images of glass impinger and NGI particle sizing instruments
A) Image of the two-stage glass impinger. The upper chamber that captures aerosol droplets > 6.4 μm is denoted with a circle. The lower chamber that captures aerosol droplets < 6.4 μm is denoted with a triangle.
B) Image of the stainless steel Next Generation Impactor (NGI) that consists of 8 chambers (labeled). From left to right, the aerosol droplet size that is captured by each chamber decreases, with chamber 1 collecting droplets up to 14.10 μm and chamber 8 collecting droplets as small as 0.24 μm.

Reprinted from Hickey, A. J. & Stewart, I. E. Inhaled antibodies: Quality and performance considerations. *Hum. Vaccin. Immunother*. 1–10 (2021).; used with permission

2.3.2 Structural and molecular changes of ACE2-linker-Fc post nebulization

First, we aimed to assess if the ACE2-linker-Fc molecule underwent any structural changes on a molecular or physical level due to nebulization. To assess this, we carried out Native-PAGE on post-nebulized ACE2-linker-Fc and compared these samples to ACE2-linker-Fc that had not undergone nebulization. For both nebulization concentrations (10 mg/mL and 20 mg/mL) and for both collection vessels (glass impinger and NGI), all proteins ran as a single band at an anticipated ~350 kDa MW and showed no observable differences between nebulized

and non-nebulized samples (Figure 2.2). It is important to note that in the instance of the 20 mg/mL nebulization into the NGI, we have proceeded only with assaying sample recovered from chambers 2-5, as those are the chambers where appreciable protein concentration was recovered (with other chambers possessing <0.08 mg/mL of the protein). The Native-PAGE also served to show that there was no detectable aggregation of the protein post-nebulization, which was somewhat expected, as VMNs nebulize mAbs with significantly less aggregates, but was still an encouraging result to see[53].

Our ACE2-linker-Fc molecule was able to undergo nebulization without accruing changes in its molecular or physical structure, and – equally as important – without causing aggregates. These results are promising, as it seems that nebulization via VMN does not significantly affect the protein in a way that compromises its architecture or design.

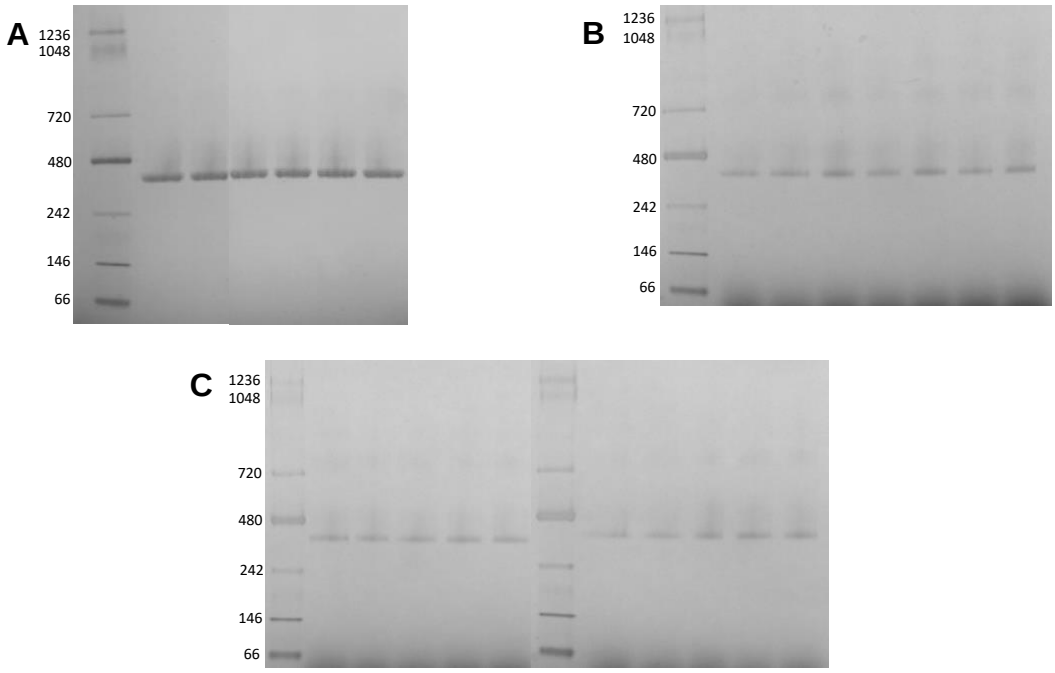

Figure 2.2 Native-PAGE of nebulized ACE2-linker-Fc
A) Native-PAGE of ACE2-linker-Fc that was nebulized at 10 mg/mL into a glass impinger. The values on the left designate MW in kDa. From left to right, the lanes are as follows: ladder, upper^{A}, lower^{A}, upper^{B}, lower^{B}, upper^{C}, lower^{C}. The "upper" and "lower" refers to which chamber the molecule was nebulized into and recovered from, and the superscript letter refers to the corresponding run, with n=3 (A, B, C) number of runs performed. The proteins ran at ~350 kDa and showed no signs of aggregation or structural changes.
B) Native-PAGE of ACE2-linker-Fc that was nebulized at 20 mg/mL into a glass impinger. The values on the left designate MW in kDa. From left to right, the lanes are as follows: ladder, unnebulized ACE2-linker-Fc, upper^{A}, lower^{A}, upper^{B}, lower^{B}, upper^{C}, lower^{C}. The "upper" and "lower" refers to which chamber the molecule was nebulized into and recovered from, and the superscript letter refers to the corresponding run, with n=3 (A, B, C) number of runs performed. The proteins ran at ~350 kDa and showed no signs of aggregation or structural changes. The nebulized protein also did not display any discernible difference to the non-nebulized protein.
C) Two Native-PAGEs of ACE2-linker-Fc that was nebulized at 20 mg/mL into an NGI. The values on the left designate MW in kDa. From left to right, the samples are as follows: ladder, unnebulized ACE2-linker-Fc, 2^{A}, 3^{A}, 4^{A}, 5^{A}, ladder, unnebulized ACE2-linker-Fc, 2^{B}, 3^{B}, 4^{B}, 5^{B}. The number (2-5) refers to which chamber the molecule was nebulized into and recovered from, and the superscript letter refers to the corresponding run, with n=3 (A, B, C) number of runs performed (run C not shown). The proteins ran at ~350 kDa and showed no signs of aggregation or structural changes. The nebulized protein also did not display any discernible difference to the non-nebulized protein.

2.3.3 Binding affinity of ACE2-linker-Fc post nebulization

Now that we had confirmed that ACE2-linker-Fc retains its structure after being nebulized, we next wished to determine if post-nebulized ACE2-linker-Fc maintained its binding affinity, as well. To ascertain this, ELISAs were performed on the same samples that had been analyzed with Native-PAGE. Across both nebulization concentrations and both collection vessels, EC_{50}s of post-nebulized ACE2-linker-Fc was comparable to EC_{50}s of ACE2-linker-Fc that had not been nebulized (Figure 2.3). For ACE2-linker-Fc that had been nebulized into a glass impinger at 10 mg/mL, the median EC_{50}s for the non-nebulized protein, protein recovered from the upper chamber, and protein recovered from the lower chamber were 0.16 nM, 0.29 nM, and 0.15 nM, respectively (SD=0.06 nM) (Figure 2.3B), while the median EC_{50}s for the 20 mg/mL run were 0.80 nM, 1.04 nM, and 0.90 nM, respectively (SD=0.10 nM) (Figure 2.3D). For ACE2-linker-Fc that had been nebulized into an NGI at a 20 mg/mL concentration, the median EC_{50}s for non-nebulized protein, protein recovered from chamber 2, chamber 3, chamber 4, and chamber 5 were 0.87 nM, 0.79 nM, 0.57 nM, 0.71 nM, and 0.74 nM, respectively (SD=0.10 nM) (Figure 2.3F).

The ACE2-linker-Fc molecule manages to retain its high binding affinity following nebulization, and at high nebulization concentrations, as well. These results are promising, in that they strongly suggest that ACE2-linker-Fc can be delivered via nebulization at high concentrations, and the nebulized protein will retain its high binding affinity, thus being a promising, efficient treatment of SARS-CoV-2.

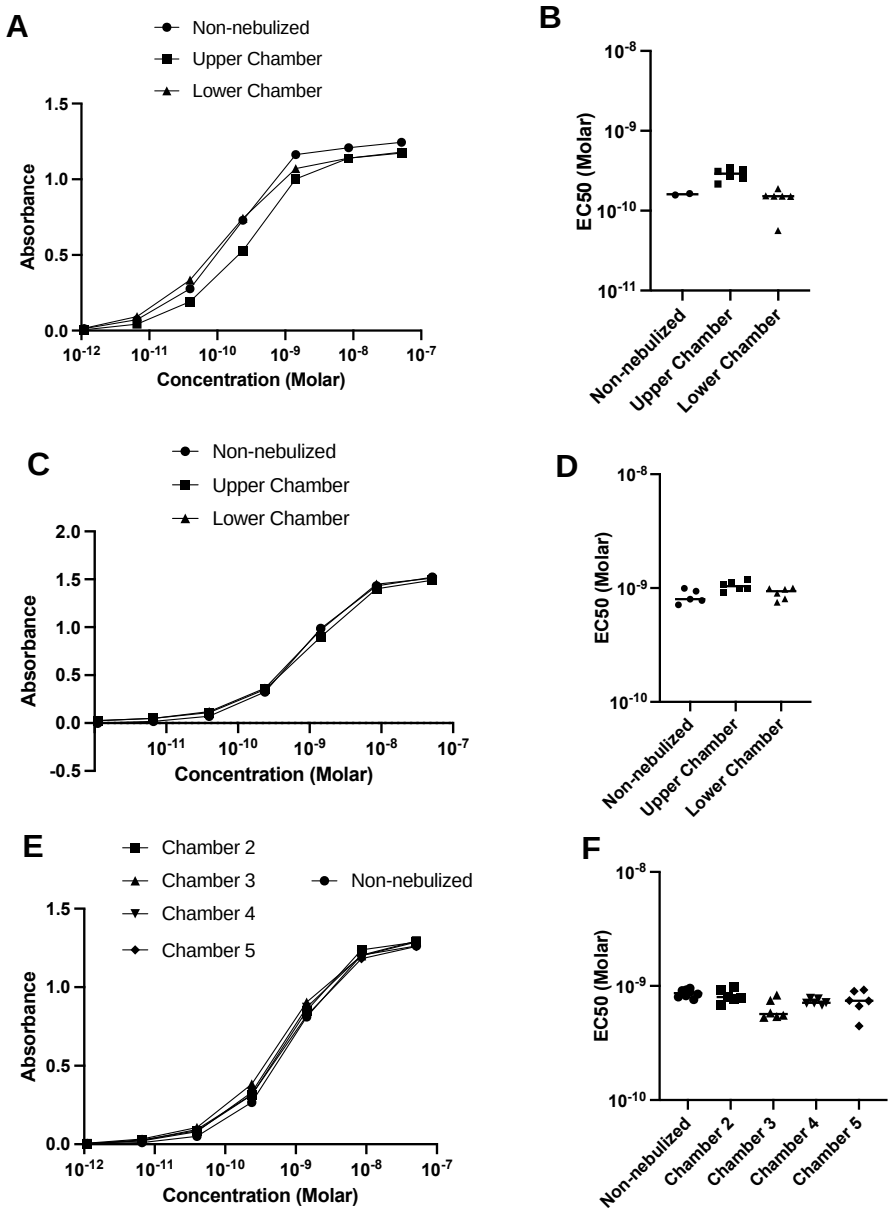

Figure 2.3 ELISA binding curves and EC_{50}s of nebulized ACE2-linker-Fc
A) ELISA binding curves of non-nebulized and nebulized ACE2-linker-Fc binding to WT S protein. Displayed is ACE2-linker-Fc nebulized at 10 mg/mL into a glass impinger, either in the upper or lower chamber.
B) EC_{50}s of ELISA binding assays from (A) are plotted, with the median EC_{50} designated with a line. The median EC_{50}s for non-nebulized ACE2-linker Fc, ACE2-linker-Fc from upper chamber, and ACE2-linker-Fc from lower chamber are 0.16 nM, 0.29 nM, and 0.15 nM, respectively. The SD is 0.06 nM.
C) ELISA binding curves of non-nebulized and nebulized ACE2-linker-Fc binding to WT S protein. Displayed is ACE2-linker-Fc nebulized at 20 mg/mL into a glass impinger, either in the upper or lower chamber.
D) EC_{50}s of ELISA binding assays from (C) are plotted, with the median EC_{50} designated with a line. The median EC_{50}s for non-nebulized ACE2-linker Fc, ACE2-linker-Fc from upper

chamber, and ACE2-linker-Fc from lower chamber are 0.80 nM, 1.04 nM, and 0.90 nM, respectively. The SD is 0.10 nM.
E) ELISA binding curves of non-nebulized and nebulized ACE2-linker-Fc binding to WT S protein. Displayed is ACE2-linker-Fc nebulized at 20 mg/mL into an NGI, in chambers 2, 3, 4, or 5.
F) EC_{50}s of ELISA binding assays from (E) are plotted, with the median EC_{50} designated with a line. The median EC_{50}s for non-nebulized ACE2-linker Fc, ACE2-linker-Fc from chamber 2, chanber 3, chamber 4, and chamber 5 are 0.87 nM, 0.79 nM, 0.57 nM, 0.71 nM, and 0.74 nM, respectively. The SD is 0.10 nM.

2.4 Discussion

We have shown here in this chapter a potentially highly effective, convenient, and applicable administration method of the ACE2-linker-Fc molecule. The molecule is able to be nebulized via a commercial vibrating mesh nebulizer, and the resulting post-nebulized protein retains its molecular and physical structure as well as its strong binding affinity to the SARS-CoV-2 S protein, without aggregation of the molecule occurring (a common concern involved in protein nebulization).

The nebulization, or inhaled delivery, approach provides several major advantages when examined in the treatment of respiratory diseases. Chiefly, inhaled delivery directly to the lung maximizes the concentration of the protein therapeutic in the respiratory tract. This primary benefit of inhaled local delivery minimizes the dosage that would be required for systemic administration, since the amount of systemically dosed mAb that ends up in the respiratory tract is usually only a small fraction[57]. Thus, for the same amount of protein, utilizing local delivery of the therapeutic to the respiratory tract can treat at least 4x more patients compared to using systemic delivery, while also providing higher protein concentration at the target location, the lungs[18,57]. These factors will allow for more patients to be treated in shorter periods of time, as well as alleviate the cost burden for such therapeutics.

Inhaled administration of protein therapeutics also allows for the maximum concentration of the drug (C_{max}) in the respiratory tract to be achieved almost immediately, whereas it can take several hours to days for C_{max} to be achieved when administered intravenously[58]. Furthermore, nebulization can be easily carried out by the patients themselves in their own homes, which can greatly mitigate the strain that is currently presented to healthcare workers and the entire healthcare infrastructure.

In addition to these general advantages that accompany inhaled delivery, our ACE2-linker-Fc molecule benefits from inhaled administration to an even greater extent, due to its structural design. As described in the previous chapter, the Fc portion of our molecule serves to allow for "muco-trapping" of the SARS-CoV-2 virus to occur, where an array of Fcs facilitates trapping of the virus in airway mucus (AM), due to the weak affinity of Fc to the mucins that make up AM[28-30]. These "trapped" viruses are then expelled out via natural mucociliary actions or through coughing[28]. The SARS-CoV-2 virus infects the apical side of airway epithelium (the airway lumen) and mainly sheds progeny viruses back into the AM that coats the epithelium[27]. Thus, it is beneficial to utilize inhaled delivery to distribute the protein therapeutic directly to the location where the infection is actively occurring and spreading.

In the past decade, vibrating mesh nebulizers (VMNs) have increasingly become the preferred method of therapeutic nebulization, with VMNs being utilized in 60% of registered clinical trials in the USA and EU between 2006 and 2016[37]. Breath-activated, or "smart" functions have further increased the efficacy of VMNs, as well. One "smart" technology that has been integrated into VMNs is adaptive aerosol delivery (AAD), which predicts the patient's inhalation pattern to optimize the aerosol delivery time, which then decreases the amount of drug waste that is exhaled[59]. Delivery via VMNs have also shown promise in several preclinical

studies, where nebulized proteins display no aggregation or degradation and also retain their high affinity and potency[60]. It's also been shown that IgG, IgA, and even a large molecule such as IgM can be successfully deposited into the lungs of rats and non-human primates utilizing a VMN[61].

In vivo work is needed in order to more accurately assess the benefits and practicality of nebulization in a living organism. For instance, in *in vivo* data that was briefly discussed in the last chapter (carried out by our group and to be submitted for publication soon), it was shown that ACE2-linker-Fc was able to effectively suppress SARS-CoV-2 in the nasal turbinate of hamsters, however, there was only a limited anti-viral effect seen in the lung[18]. It is hypothesized that the minimal effect observed in the lung may be due to non-uniform distribution of ACE2-linker-Fc from intranasal delivery, and that this issue may be resolved by utilizing a vibrating mesh nebulizer, since it provides more uniform delivery across the respiratory tract[18]. Indeed, it will be valuable and interesting to observe the results of *in vivo* nebulization experiments of ACE2-linker-Fc, since the conclusions thus far appear to be incredibly promising.

REFERENCES

1. WHO Coronavirus (COVID-19) Dashboard. *World Health Organization* https://covid19.who.int/ (2021)

2. Bernal, J. L. *et al.* Effectiveness of Covid-19 Vaccines against the B.1.617.2 (Delta) Variant. *New England Journal of Medicine* vol. 385 585–594 (2021)

3. Dieterle, M. E. *et al.* A Replication-Competent Vesicular Stomatitis Virus for Studies of SARS-CoV-2 Spike-Mediated Cell Entry and Its Inhibition. *Cell Host Microbe* **28**, 486–496.e6 (2020)

4. Bosch, B. J., van der Zee, R., de Haan, C. A. M. & Rottier, P. J. M. The coronavirus spike protein is a class I virus fusion protein: structural and functional characterization of the fusion core complex. *J. Virol.* **77**, 8801–8811 (2003)

5. Shang, J. *et al.* Cell entry mechanisms of SARS-CoV-2. *Proc. Natl. Acad. Sci. U. S. A.* **117**, 11727–11734 (2020)

6. Higuchi, Y., Suzuki, T., Arimori, T., Ikemura, N. & Kirita, Y. High affinity modified ACE2 receptors prevent SARS-CoV-2 infection. *BioRxiv* (2020)

7. Chan, K. K. *et al.* Engineering human ACE2 to optimize binding to the spike protein of SARS coronavirus 2. *Science* **369**, 1261–1265 (2020)

8. Tada, T. *et al.* An ACE2 Microbody Containing a Single Immunoglobulin Fc Domain Is a Potent Inhibitor of SARS-CoV-2. *Cell Rep.* **33**, 108528 (2020)

9. Glasgow, A. *et al.* Engineered ACE2 receptor traps potently neutralize SARS-CoV-2. *Proc. Natl. Acad. Sci. U. S. A.* **117**, 28046–28055 (2020)

10. Iwanaga, N. *et al.* Novel ACE2-IgG1 fusions with improved in vitro and in vivo activity against SARS-CoV2. doi:10.1101/2020.06.15.152157

11. Lei, C. *et al.* Neutralization of SARS-CoV-2 spike pseudotyped virus by recombinant ACE2-Ig. *Nat. Commun.* **11**, 2070 (2020)

12. Tanaka, S. *et al.* A recombinant 'ACE2 Triple Decoy' that traps and neutralizes SARS-CoV-2 shows enhanced affinity for highly transmissible SARS-CoV-2 variants. doi:10.1101/2021.03.09.434641

13. Miller, A. *et al.* A super-potent tetramerized ACE2 protein displays enhanced neutralization of SARS-CoV-2 virus infection. *Sci. Rep.* **11**, 10617 (2021)

14. Huang, K.-Y. *et al.* Humanized COVID-19 decoy antibody effectively blocks viral entry and prevents SARS-CoV-2 infection. *EMBO Mol. Med.* **13**, e12828 (2021)

15. Wysocki, J. *et al.* A Novel Soluble ACE2 Variant with Prolonged Duration of Action Neutralizes SARS-CoV-2 Infection in Human Kidney Organoids. *J. Am. Soc. Nephrol.* (2021) doi:10.1681/ASN.2020101537

16. Xiao, T. *et al.* A trimeric human angiotensin-converting enzyme 2 as an anti-SARS-CoV-2 agent in vitro. *bioRxiv* (2020) doi:10.1101/2020.09.18.301952

17. Neuman, B. W. *et al.* Supramolecular architecture of severe acute respiratory syndrome coronavirus revealed by electron cryomicroscopy. *J. Virol.* **80**, 7918–7928 (2006)

18. Tiruthani, K. *et al.* Engineering a "muco-trapping" ACE2-immunoglobulin hybrid with picomolar affinity for topical immunotherapy against SARS-CoV-2. To be submitted.

19. Planas, D. *et al.* Sensitivity of infectious SARS-CoV-2 B.1.1.7 and B.1.351 variants to neutralizing antibodies. *Nat. Med.* **27**, 917–924 (2021)

20. Moore, M. J. *et al.* Retroviruses pseudotyped with the severe acute respiratory syndrome coronavirus spike protein efficiently infect cells expressing angiotensin-converting enzyme 2. *J. Virol.* **78**, 10628–10635 (2004)

21. Edara, V. V. *et al.* Reduced binding and neutralization of infection- and vaccine-induced antibodies to the B.1.351 (South African) SARS-CoV-2 variant. doi:10.1101/2021.02.20.432046

22. Baum, A. *et al.* Antibody cocktail to SARS-CoV-2 spike protein prevents rapid mutational escape seen with individual antibodies. *Science* **369**, 1014–1018 (2020)

23. Japan Becomes First Country to Approve Regenron Antibody Cocktail (Casirivimab and Imdevimab) for the Treatment of Mild to Moderate COVID-19. *Regeneron Pharmaceuticals, Inc* https://newsroom.regeneron.com/news-releases/news-release-details/japan-becomes-first-country-approve-regeneron-antibody-cocktail#:~:text=00%20AM%20EDT-,Japan%20Becomes%20First%20Country%20to%20Approve%20Regeneron%20Antibody%20Cocktail%20(casirivimab,%2F%20%2D%2D%20Regeneron%20Pharmaceuticals%2C%20Inc (2021)

24. Izquierdo-Useros, N. *et al.* Capture and transfer of HIV-1 particles by mature dendritic cells converges with the exosome-dissemination pathway. *Blood* vol. 113 2732–2741 (2009)

25. Starr, T. N. *et al.* Prospective mapping of viral mutations that escape antibodies used to treat COVID-19. doi:10.1101/2020.11.30.405472

26. Guo, L. *et al.* Engineered Trimeric ACE2 Binds and Locks 'Three-up' Spike Protein to Potently Inhibit SARS-CoVs and Mutants. doi:10.1101/2020.08.31.274704

27. Milewska, A. *et al.* Replication of SARS-CoV-2 in human respiratory epithelium. doi:10.1101/2020.03.20.999029

28. Yang, B. *et al.* ZMapp Reinforces the Airway Mucosal Barrier Against Ebola Virus. *J. Infect. Dis.* **218**, 901–910 (2018)

29. Wang, Y.-Y. *et al.* IgG in cervicovaginal mucus traps HSV and prevents vaginal herpes infections. *Mucosal Immunol.* **7**, 1036–1044 (2014)

30. Newby, J. *et al.* A blueprint for robust crosslinking of mobile species in biogels with weakly adhesive molecular anchors. *Nature Communications* vol. 8 (2017)

31. Matthews, A. A., Ee, P. L. R. & Ge, R. Developing inhaled protein therapeutics for lung diseases. *Molecular Biomedicine* **1**, 11 (2020)

32. Respaud, R., Vecellio, L., Diot, P. & Heuzé-Vourc'h, N. Nebulization as a delivery method for mAbs in respiratory diseases. *Expert Opin. Drug Deliv.* **12**, 1027–1039 (2015)

33. Morishita, M. & Peppas, N. A. Is the oral route possible for peptide and protein drug delivery? *Drug Discov. Today* **11**, 905–910 (2006)

34. Matucci, A., Vultaggio, A. & Danesi, R. The use of intravenous versus subcutaneous monoclonal antibodies in the treatment of severe asthma: a review. *Respir. Res.* **19**, 154 (2018)

35. Borghardt, J. M., Kloft, C. & Sharma, A. Inhaled Therapy in Respiratory Disease: The Complex Interplay of Pulmonary Kinetic Processes. *Can. Respir. J.* **2018**, 2732017 (2018)

36. Koussoroplis, S. J. *et al.* PEGylation of antibody fragments greatly increases their local residence time following delivery to the respiratory tract. *J. Control. Release* **187**, 91–100 (2014)

37. Cruz-Teran, C. *et al.* Challenges and opportunities for antiviral monoclonal antibodies as COVID-19 therapy. *Adv. Drug Deliv. Rev.* **169**, 100–117 (2021)

38. Hickey, A. J. Controlled delivery of inhaled therapeutic agents. *J. Control. Release* **190**, 182–188 (2014)

39. Niven, R. W. Delivery of biotherapeutics by inhalation aerosol. *Crit. Rev. Ther. Drug Carrier Syst.* **12**, 151–231 (1995)

40. Morales, J. O. *et al.* Challenges and Future Prospects for the Delivery of Biologics: Oral Mucosal, Pulmonary, and Transdermal Routes. *AAPS J.* **19**, 652–668 (2017)

41. Narang, A. S., Krause, M. E., Pizarro, S. & Yee, J. C. Biologic Drug Substance and Drug Product Manufacture. in *Pharmaceutical Inhalation Aerosol Technology* 205–232 (CRC Press, 2019).

42. Hertel, S., Pohl, T., Friess, W. & Winter, G. That's cool!–Nebulization of thermolabile proteins with a cooled vibrating mesh nebulizer. *Eur. J. Pharm. Biopharm.* (2014)

43. United States Pharmacopeial Convention. Products for Nebulization – Characterization Tests. in *USP 35 NF30, 2012: U.S. Pharmacopoeia National Formulary* 942-945 (United States Pharmacopeial, 2011).

44. Lip Kwok, P. C. & Chan, H. K. Chapter 2--Pulmonary Delivery of Peptides and Proteins. (2011)

45. Kane, C., O'Neil, K., Conk, M. & Picha, K. Inhalation delivery of protein therapeutics. *Inflamm. Allergy Drug Targets* **12**, 81–87 (2013)

46. Carvalho, T. C., Peters, J. I. & Williams, R. O., 3rd. Influence of particle size on regional lung deposition--what evidence is there? *Int. J. Pharm.* **406**, 1–10 (2011)

47. Fängmark, I. & Carpin, J. C. Protein nebulization. *J. Aerosol Sci.* **27**, S231 (1996)

48. Hertel, S. P., Winter, G. & Friess, W. Protein stability in pulmonary drug delivery via nebulization. *Adv. Drug Deliv. Rev.* **93**, 79–94 (2015)

49. Fahy, J. V. *et al.* Effect of aerosolized anti-IgE (E25) on airway responses to inhaled allergen in asthmatic subjects. *Am. J. Respir. Crit. Care Med.* **160**, 1023–1027 (1999)

50. Clay, M. M., Pavia, D., Newman, S. P., Lennard-Jones, T. & Clarke, S. W. Assessment of jet nebulisers for lung aerosol therapy. *Lancet* **2**, 592–594 (1983)

51. McCarthy, S. D., González, H. E. & Higgins, B. D. Future Trends in Nebulized Therapies for Pulmonary Disease. *J Pers Med* **10**, (2020)

52. Bohr, A. & Beck-Broichsitter, M. Generation of tailored aerosols for inhalative drug delivery employing recent vibrating-mesh nebulizer systems. *Ther. Deliv.* **6**, 621–636 (2015)

53. Maillet, A. *et al.* Aerodynamical, immunological and pharmacological properties of the anticancer antibody cetuximab following nebulization. *Pharm. Res.* **25**, 1318–1326 (2008)

54. Kuo, Y.-M., Chan, W.-H., Lin, C.-W., Huang, S.-H. & Chen, C.-C. Characterization of vibrating mesh aerosol generators. *Aerosol Air Qual. Res.* **19**, 1678–1687 (2019)

55. Hickey, A. J. & Stewart, I. E. Inhaled antibodies: Quality and performance considerations. *Hum. Vaccin. Immunother.* 1–10 (2021)

56. Marple, V. A. *et al.* Next generation pharmaceutical impactor (a new impactor for pharmaceutical inhaler testing). Part I: Design. *J. Aerosol Med.* **16**, 283–299 (2003)

57. Dall'Acqua, W. F., Kiener, P. A. & Wu, H. Properties of human IgG1s engineered for enhanced binding to the neonatal Fc receptor (FcRn). *J. Biol. Chem.* **281**, 23514–23524 (2006)

58. Yapa, S. W. S. *et al.* Pulmonary and Systemic Pharmacokinetics of Inhaled and Intravenous Colistin Methanesulfonate in Cystic Fibrosis Patients: Targeting Advantage of Inhalational Administration. *Antimicrobial Agents and Chemotherapy* vol. 58 2570–2579 (2014)

59. Denyer, J., Nikander, K. & Smith, N. J. Adaptive Aerosol Delivery (AAD®) technology. *Expert Opin. Drug Deliv.* **1**, 165–176 (2004)

60. Lightwood, D. *et al.* The discovery, engineering and characterisation of a highly potent anti-human IL-13 fab fragment designed for administration by inhalation. *J. Mol. Biol.* **425**, 577–593 (2013)

61. Vonarburg, C. *et al.* Topical application of nebulized human IgG, IgA and IgAM in the lungs of rats and non-human primates. *Respir. Res.* **20**, 99 (2019)